

Reflux condensation synthesis and characterization of Co_3O_4 nanoparticles for photocatalytic applications

M. Mohamed Jaffer Sadiq^a, A. Samson Nesaraj^{b,*}

^aDepartment of Nanosciences and Technology, School of Science & Humanities, Karunya University, Karunya Nagar, Coimbatore -641114, India.

^bDepartment of Chemistry, Karunya University, School of Science & Humanities, Karunya Nagar, Coimbatore-641114, India.

Received 23 September 2014; received in revised form 19 October 2014; accepted 22 October 2014

ABSTRACT

In this research work, we report a simple method called reflux condensation method for synthesizing Co_3O_4 nanoparticles using cheap chemicals such as, cobalt acetate (precursor salt), sodium monododecyl sulphate - SDS (surfactant) and N, N - Dimethylformamide - DMF (solvent). The prepared materials were heat treated at 200, 400, 600 and 800 °C for each 2 h to get phase pure product. The calcined nanoparticles were characterized by XRD, EDAX, FTIR Spectroscopy, Particle Size Analysis, SEM, UV-Vis Spectroscopy (UV) and Photo Luminescence (PL) Spectroscopy techniques. The XRD data confirmed the presence of crystallization of Co_3O_4 nanoparticles as face-centered cubic (Fd3m) structure. The appearance of Co-O stretching vibration mode and bridging vibration of O-Co-O bond in the samples found out by FTIR spectroscopy. The particulate and microstructural studies revealed the occurrence of nanoparticles in the samples. The atomic percentages of Co and O were found to be 42% and 58% in the sample. This energy band gap for the sample is found to be 5.6 eV. Photocatalytic degradation characteristics of methyl orange and Rhodamine B using Co_3O_4 nanoparticles were studied and reported. Among the two dye samples studied, methyl orange was found to be degraded effectively (76%) with Co_3O_4 nanoparticles in presence of UV-light after two hours of irradiation.

Keywords: Co_3O_4 nanoparticles, Reflux condensation method, Characterization, Photocatalytic studies.

1. Introduction

In recent years, the use of metal oxides as photocatalysts for degradation of organic substances has attracted attention of scientific community. Metal oxide nanoparticles have been studied due to their novel optical, electronic, magnetic, thermal and potential application in catalyst, gas-sensors and photo-electronic devices. In the present scenario, the environment is deeply polluted in various ways because of rapid urbanization in developing countries. The concept of urbanization includes high level settlement of humans, industrialization, huge transport, etc. in urban areas. Among the various types of pollution reported in the literature, water pollution can affect the living things present in the environment in a greater extent. Especially, the wastewater with noxious organic dyes discharged by various industries such as

textiles, plastics, paper, paint, cosmetics are great hazard to the ambient ecosystem now-a-days [1,2]. The removal of these organic compounds is a major concern in ensuring a safe and healthy environment. The semiconductor photocatalysts offer an extremely convenient route for eliminating the water pollution as well as various organic pollutants by UV or solar light irradiation in the presence of photocatalysts [3,4]. Nanostructured materials have attracted the attention of researchers due to their interesting properties, promising applications in various fields of the transition metal oxides [5-9]. Cobalt oxides are of the most versatile materials from the transition-metal oxides compounds and it was stable in normal environment condition. Nanostructured cobalt oxide is a p-type semiconductor and it has direct energy band gap in between 1.5-2.0 eV [10]. It has an antiferromagnetic property and its crystal structure is spinel (Fd3m) based on a cubic close packing array of oxide ions [11]. In addition to that, these materials are having good magnetic, optical and transport properties

*Corresponding author email: drsamson@karunya.edu
Tel.: +91 98 9472 3178

on the nanoscale region [12]. Cobalt oxide (Co_3O_4) finds enormous applications in rechargeable battery [13], heterogeneous catalysts [14], magnetic materials [15], gas sensors [16], solar energy absorbers [17], supercapacitors [18], phosphate ion sensors [19], optical sensors [20], solid-state sensors [21], super hydrophobic surfaces [22], electro chromic sensors [23], energy storage [24] and pigments [25]. Recently, several methods have been developed for the preparation of cobalt oxides such as microwave-assisted hydrothermal method [20], ultrasonic-assisted hydrothermal process [22], sol-gel method [26], hydrothermal method [27], combustion method [28], micro emulsion method [29], chemical spray pyrolysis [30], chemical vapor deposition [31], thermal decomposition [32], sonochemical route [33], microwave irradiation [34], mechano-chemical processing [35], soft chemical method [36] and molten salt approach process [37]. Both pure cobalt oxide and cobalt oxide based composites such as, $\text{Co}_3\text{O}_4\text{-Al}_2\text{O}_3$, $\text{Co}_3\text{O}_4\text{-SiO}_2$, $\text{Co}_3\text{O}_4\text{-TiO}_2$ and $\text{Co}_3\text{O}_4\text{-ZnO}$ were studied for the photodegradation of methyl orange, 2,4-dichlorophenol, rhodamine B etc., and showed better degradation results [38-42].

In this study, photocatalytic degradation of rhodamine B and methyl orange dye was investigated using synthesized cobalt oxide nanoparticles in presence of UV light. The prepared nanoparticles were characterized by XRD, FTIR, particle size analysis, SEM-EDAX, UV-Vis and PL techniques.

2. Experimental

2.1. Materials

The analytical grade chemicals such as Cobalt (II) acetate tetra hydrate (98.0% purity, Sigma-Aldrich, India), N, N-Dimethylformamide (99.8% purity, Merck, India), SDS (> 99% purity, Merck, India), Methyl Orange (>98.0% purity, Merck, India), Rhodamine B (>95.0% purity, Sigma-Aldrich, India) and Ethanol (99.0% purity, Merck, India) were used in this study. These materials were used as received without any further purification. All reactions were carried out by using deionized water.

2.2. Synthesis of Co_3O_4 nanoparticles

The Co_3O_4 nanoparticles were prepared by reflux condensation method. In the typical experiment, 12.4540 g cobalt acetate and 1.0 g SDS were dissolved in 100 ml DMF solvent medium. SDS was chosen as

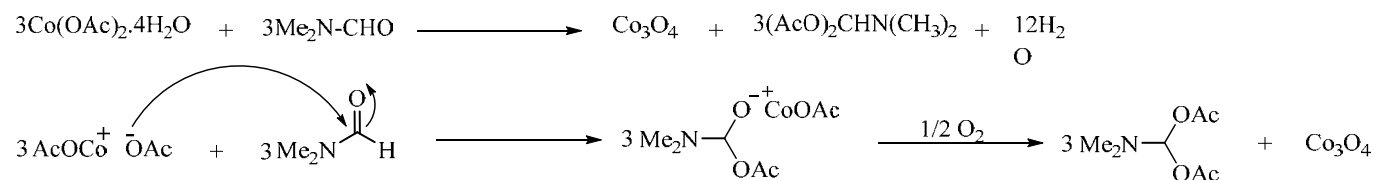
surfactant for this study based on their excellent characteristics as surfactant. The above solution mixture was then taken in a Round Bottom (RB) flask and refluxed at 90°C for 6 h in a magnetic stirring apparatus (1200 rpm). The resulting colloidal precipitate was centrifuged and washed with 10% ethanol solution. Finally, the product was dried at 85°C for 2 h and calcined at 200, 400, 600 and 800°C for 2 h each to get a phase pure product. The reaction mechanisms involved in the synthesis of Co_3O_4 nanoparticles are indicated below (Scheme 1).

2.3. Characterization

The powder XRD studies were carried out with a Shimadzu XRD6000 X-ray diffractometer using $\text{CuK}\alpha$ radiation ($\lambda = 0.154059\text{ nm}$) radiation with a nickel filter. The applied voltage and current were 40 kV and 30 mA respectively. The 2θ scanning range was chosen in the range of 30° to 90° with a scan rate of 10° min^{-1} . The crystallite sizes of cobalt oxide were calculated by using the Debye-Scherrer equation. The FTIR spectra of Co_3O_4 nano powder was recorded by Fourier transform infrared spectrometer (SHIMADZU Spectrophotometer) using KBr pellet technique in the range from 4000 cm^{-1} to 400 cm^{-1} (spectral resolution was 4 cm^{-1} and number of scans was 20). The average particle size of the Co_3O_4 nanoparticles was measured with a Zetasizer Ver. 6.32 manufactured by the Malvern Instruments Ltd. The surface morphology, size of particles and elemental compositions of Co_3O_4 nanoparticles were characterized by scanning electron microscope (SEM JEOL JSM-6610) equipped with an energy dispersive X-ray (EDAX) spectrophotometer and operated at 20 kV. Absorbance spectra of the Co_3O_4 nanoparticles was recorded by UV-Visible Spectrophotometer (Shimadzu 1800). The samples were loaded into a quartz cell and the absorption spectrum was recorded in the range between 200 nm to 600 nm. Photoluminescence spectrum of the Co_3O_4 nanoparticles was measured by Spectrofluorophotometer (FLUOROLOG, HORIBA YVON) with Xe laser as the excitation light source at room temperature.

2.4. Photocatalytic Measurements

In this study, the photocatalytic degradation of methyl orange (MO) and rhodamine B (RB dye) in presence of pure Co_3O_4 nanoparticles as well as in the absence of Co_3O_4 nanoparticles were carried out in a simple Pyrex photoreactor. The dye (MO or RB) with concentration



Scheme 1. Reaction mechanisms involved in the synthesis of Co_3O_4 nanoparticles by reflux condensation method.

of $1.0 \times 10^{-5} \text{M}$ was used in the present study. 10 mg of the prepared photocatalyst (Co_3O_4) was mixed with 50 ml of above dye solution and then sonicated for about 10 minutes in a sonicator in order to mix the photocatalyst properly with the dye solution. Then, the above reaction mixture was loaded in the photoreactor and again stirred for about 30 minutes in dark room to attain reaction equilibrium. The reaction mixture was exposed to UV light under continuous stirring and the optical density values of the reaction mixture were recorded at various time intervals (0, 40, 80 and 120 minutes). The degradation was monitored by measuring the absorbance spectra for the above samples using UV-Visible spectrophotometer. The absorbance of MO and RB was carried out at 465 and 554 nm wavelength, respectively.

3. Results and Discussion

3.1. X-Ray Diffraction Studies

The powder XRD pattern of Co_3O_4 nanoparticles is shown in Fig. 1. The XRD pattern of Co_3O_4 nanoparticles displays in the 2θ range between 30° to 90° . The peaks observed at (220), (311), (222), (400), (422), (511), (440), (533) and (444) were matched well with the standard values of Co_3O_4 (JCPDS No. 65-3103). The sample reported in this research work also crystallized as face-centered cubic (Fd3m) structure. No impurity peaks were observed. The lattice parameters values were calculated from 2θ values in the XRD patterns and reported in Table. 1. The as-synthesized Co_3O_4 nanoparticles may contain much more structure distortions than crystalline cobalt oxides [43]. The crystal size (D) was calculated using the Debye-Scherrer formula [44] as mentioned equation (1).

$$D = 0.91 \lambda / \beta \cos\theta \quad (1)$$

Where ' λ ' is the X-ray wavelength ($\lambda = 0.154059 \text{ nm}$ for $\text{CuK}\alpha$), ' β ' is the FWHM (full width at half maximum intensity) and ' θ ' is the Bragg's angle.

The theoretical density (D_p) [45] was calculated from the equation (2).

$$D_p = (Z * M) / (N * a^3) \text{ g.cm}^{-3} \quad (2)$$

Where 'Z' is the number of chemical species in the unit cell, 'M' is the molecular mass of the sample (g/mol), 'N' is the Avogadro's number (6.022×10^{23}) and 'a' is the lattice constant (cm).

The lattice constant [46] of cubic structure was calculated from the equation (3).

$$a = d * (h^2 + k^2 + l^2)^{1/2} \quad (3)$$

3.2. FT-IR Analysis

The FT-IR spectrum of Co_3O_4 nanoparticles is shown in Fig. 2. In the investigated region (wave numbers $4000\text{-}400 \text{ cm}^{-1}$), it showed significant absorption peaks at 3600 , 2360 , 1650 , 665 , and 569 cm^{-1} . It was noted that the bands appeared at 3600 and 1650 cm^{-1} respectively may be due to the stretching and bending vibrations of the water [47]. Also, there was a band at approximately 2360 cm^{-1} which may be due to the presence of atmospheric CO_2 [47]. Generally, the metal oxides may show absorption bands below 1000 cm^{-1} arising due inter-atomic vibrations [48]. The presence of two absorption bands at 569 and 665 cm^{-1} were assigned to Co-O stretching vibration mode and bridging vibration of O-Co-O bond which originate from the stretching vibrations of the metal-oxygen bond and confirmed the formation of Co_3O_4 spinel oxide [49]. The 569 cm^{-1} band is characteristic of the Co^{3+} in the octahedral hole vibration and the 665 cm^{-1} band is attributable to the Co^{2+} in the tetrahedral hole vibration in the spinel lattice [49].

3.3. Particle size analysis

The particle size distribution curve of Co_3O_4 nanoparticles is shown in Fig. 3. The sample (0.01g) was well dispersed in water (20 ml) for 30 minutes before the analysis. The corresponding particle size histogram obtained on Co_3O_4 possessed a narrow particle size distribution and the mean particle diameter was found to be approximately 43 nm. The mean particle size determined by particle size analyzer was very close to the average grain size calculated by the SEM. The large particle size observed in the particles may be due to the agglomeration of particles observed at high temperature treatment [50].

Table 1. The crystallographic parameters were obtained in the Co_3O_4 nanoparticles

Sample	Crystal structure	Unit cell lattice parameter 'a' (Å)	Unit cell volume (Å) ³	Theoretical density (g/cc)	Crystallite size (nm)
Standard XRD data for Co_3O_4 powder (JCPDS No. 65-3103)	Face centered cubic (Fd3m)	8.056	522.83	6.118	-
Synthesized Co_3O_4 nanoparticles	Face centered cubic (Fd3m)	8.047	521.08	6.138	2.4855

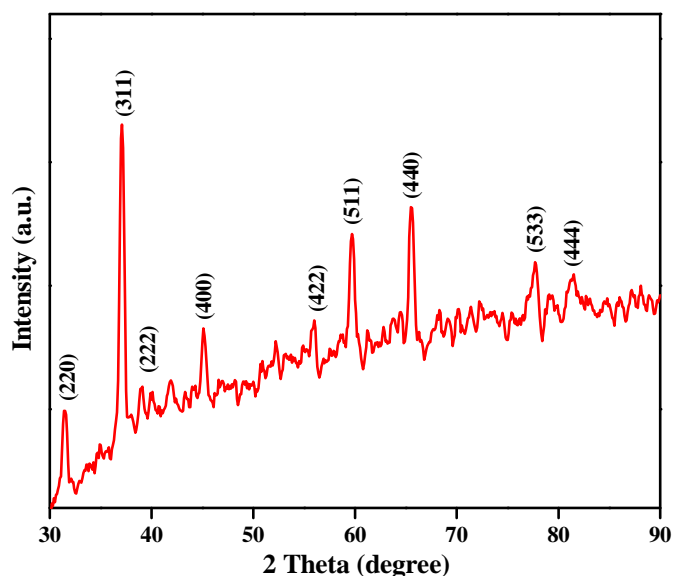


Fig. 1. The powder XRD pattern of Co_3O_4 nanoparticles.

3.4. SEM studies

The SEM image of Co_3O_4 nanoparticles is shown in Fig. 4. It can be seen that the grain size of the particles present in the range of 500 to 1 μm . In addition, spherical shaped Co_3O_4 nanoparticles with smooth surface were present in the sample. The presence of aggregation in the sample may be due to the occurrence of large surface energy and surface tension in the sample due to high temperature treatment [51].

3.5. EDAX studies

The EDAX spectrum of Co_3O_4 nanoparticles is shown in Fig. 5. The presence of Co and O in the sample was confirmed by EDAX analysis. The atomic percentages of Co and O were found to be 42% and 58% respectively. The atomic ratio of Co and O was found to be $\sim 3:3.9$, which approaches the theoretical value for Co_3O_4 .

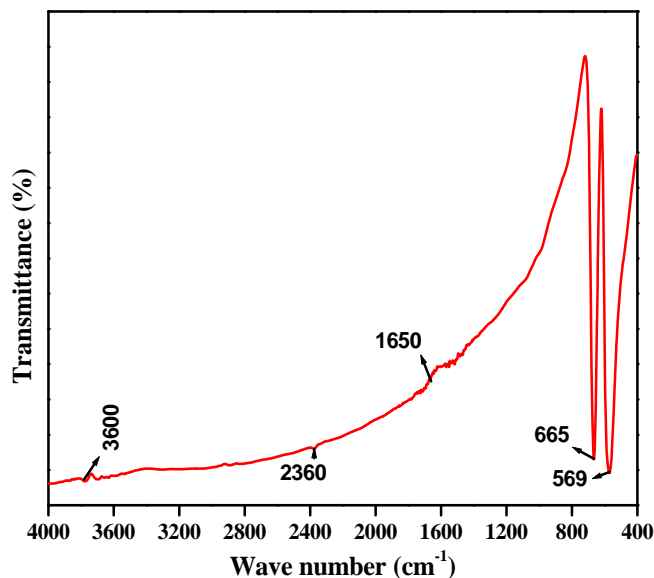


Fig. 2. The FT-IR spectrum of Co_3O_4 nanoparticles.

3.6. Optical studies

The optical absorption spectrum of Co_3O_4 nanoparticles is shown in the Fig. 6. In this spectrum absorption peak was observed at around 257 nm. Since Co_3O_4 is a p-type semiconductor, the absorption band gap (E_g) can be determined by the following Tauc [52] equation as mentioned below.

$$(\text{A}h\nu)^n = K (h\nu - E_g) \quad (4)$$

Where, ' $h\nu$ ' is the photon energy (eV), ' A ' is the absorption coefficient, ' K ' is a constant relative to the material, ' E_g ' is the band gap and ' n ' is either 1/2 for an indirect transition or 2 for a direct transition. According to the literatures [53], the obtained Co_3O_4 nanoparticles can involve in direct transition. The direct band gap can be estimated by extrapolating the linear region in the Tauc plot of $(\text{A}h\nu)^2$ versus photon energy ($h\nu$) is shown inset the Fig. 7(a).

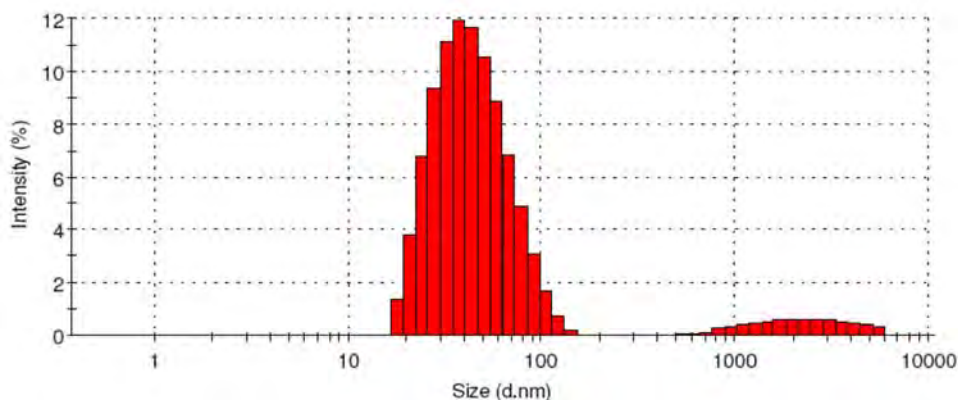


Fig. 3. The particle size distributions curve of Co_3O_4 nanoparticles.

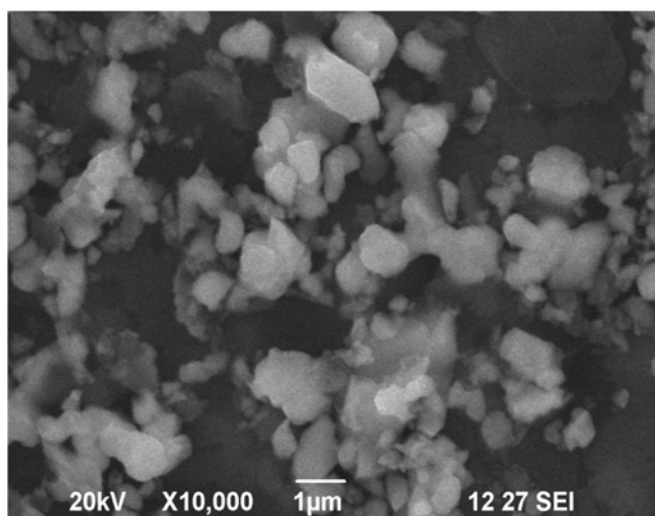


Fig. 4. The SEM image of Co_3O_4 nanoparticles.

This gives the energy band gap for the sample as 5.6 eV. From the literature, it was found that the band gap values for Co_3O_4 were found to be 1.77 - 3.17 eV [44]. The increase in the band gap value found in the prepared Co_3O_4 nanoparticles may be quantum confinement effects of nanoparticles as reported [36].

3.7. Photo Luminescence (PL) studies

The PL Emission spectrum of Co_3O_4 nanoparticles is shown in Fig. 7. According to the UV absorbance, the nanoparticle exhibits the excitation wavelength around 275 nm. The strong broad emission peaks found at 302 and 310 nm respectively in the band gap range of 4.0-4.1 eV may be due to the emission band edge and this may be due to the recombination of excitons.

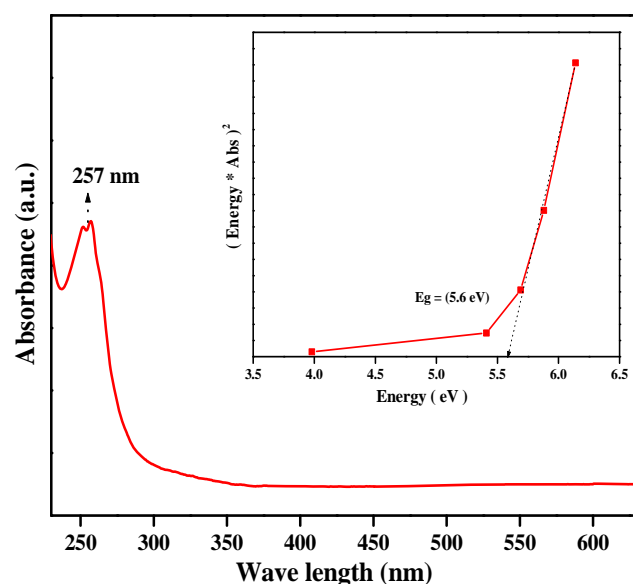


Fig. 6. The Absorbance spectrum and inset the direct band gap energy of Co_3O_4 nanoparticles.

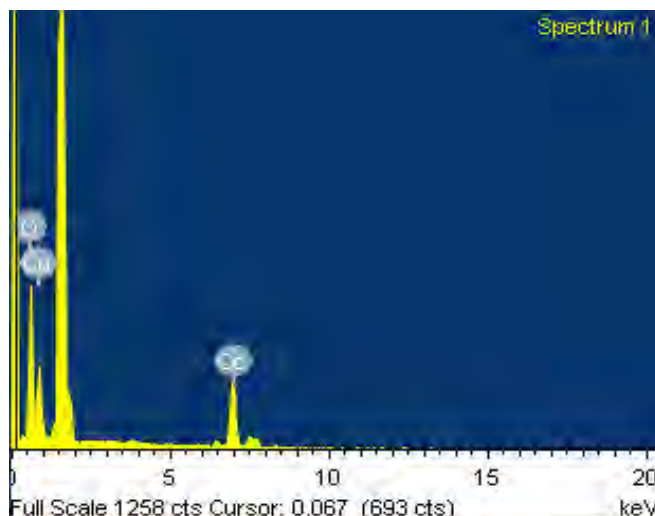


Fig. 5. The EDAX spectrum of Co_3O_4 nanoparticles.

The presence of strong broad emission peak reported in PL spectrum may also be due to the high purity and perfect crystalline nature of the Co_3O_4 nanoparticles.

3.8. Photocatalytic studies

Fig. 8 and 9 shows the UV-Vis absorption spectra of Rhodamine B and methyl orange dye when exposed to UV light of 254 nm for the time intervals such as, 0, 40, 80 and 120 min respectively in the presence of Co_3O_4 nanoparticles. It was seen that after irradiating for about 40 minutes, the absorption peak intensity decreased slowly. After that, it continuously decreased with increasing UV light exposure time. It shows that the Co_3O_4 nanoparticle has good photocatalytic degradation efficiency in UV light source.

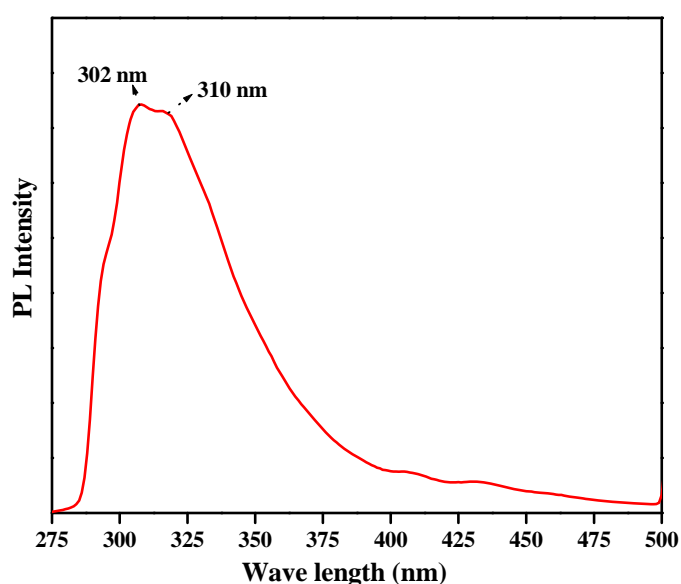


Fig. 7. The PL Emission spectrum of Co_3O_4 nanoparticles.

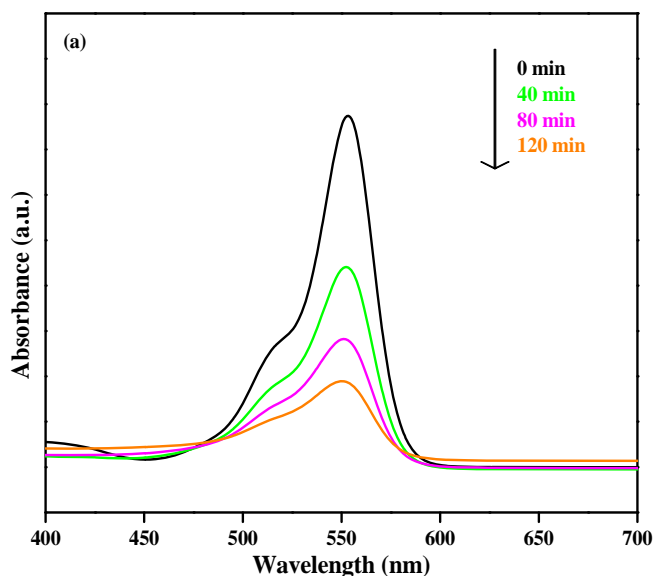


Fig. 8. Absorption spectrum of RB in Co_3O_4 nanoparticles at different interval time.

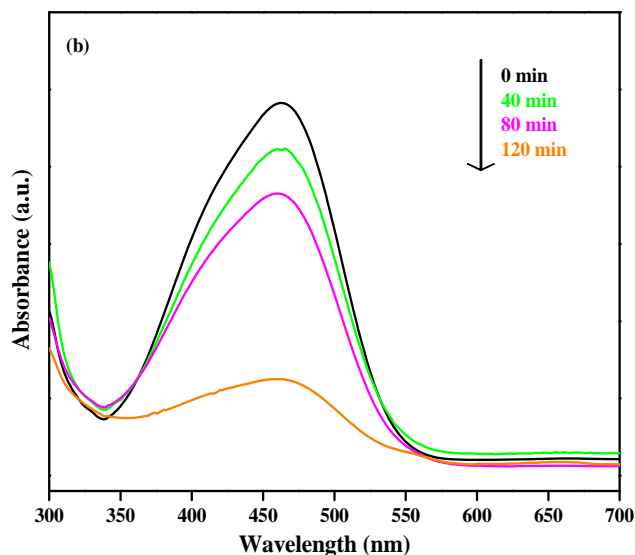


Fig. 9. Absorption spectrum of MO in Co_3O_4 nanoparticles at different interval time.

The percentage of degradation was calculated [54] from formula (5).

$$\% \text{Degradation} = ((C_0 - C_t) / C_0) \times 100 \quad (5)$$

Where, ' C_0 ' is the initial absorbance of the dye solution and ' C_t ' is the absorbance at time interval respectively.

Fig. 10 shows the degradation of methyl orange and rhodamine B in presence Co_3O_4 nanoparticles irradiated under UV light. The degradation rate of methyl orange and rhodamine B dye without catalyst was found to 18% and 23% respectively even after 120 minutes exposure to UV light.

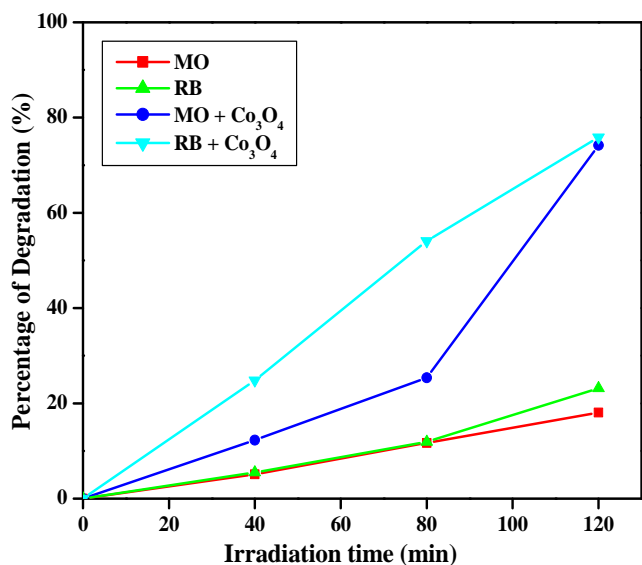


Fig. 10. The percentage of degradation with time for RB and MO dye under UV light irradiation for the presence and absence of Co_3O_4 nanoparticle.

In presence of Co_3O_4 , the dyes such as methyl orange and rhodamine B were degraded 74% and 76% respectively after exposure to UV radiation for about 120 minutes. According to literature, Co_3O_4 nanofiber based photocatalysts degraded rhodamine B only 60 % after 3 of UV exposure [44]. Both the results show a good level of decrease in the absorption intensity with respect to time. Based on our study, Co_3O_4 nanoparticle can act as a good photocatalyst especially to degrade rhodamine B than methyl orange under UV light irradiation. Photocatalytic reactions with different dyes can be expressed by the Langmuir-Hinshelwood [55] kinetics curve as indicated in Fig. 11.

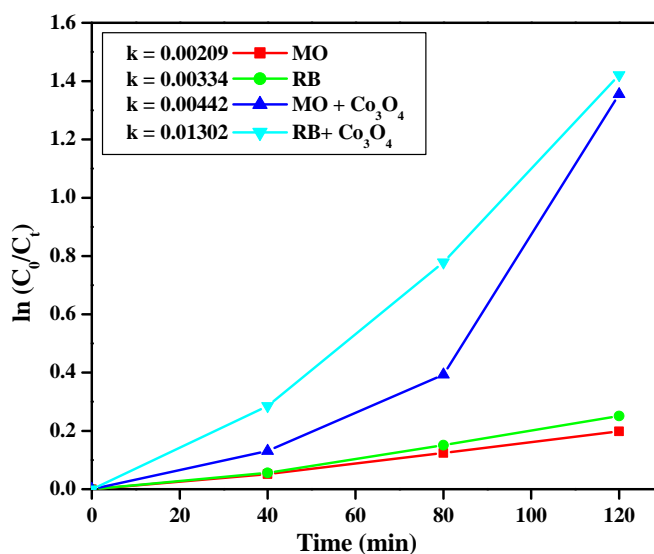


Fig. 11. Kinetic linear curves of RB and MO dye in the presence and absence of Co_3O_4 nanoparticle.

The photocatalytic degradation of methyl orange and rhodamine B with and without photocatalysts under UV light obeys pseudo-first-order kinetics with respect to the concentration of methyl orange and rhodamine B respectively [55].

$$-dc/dt = k_{app}c \quad (6)$$

Integration of this equation (with the restriction of $c = c_0$ at $t = 0$, where c_0 is the initial concentration, after dark adsorption of the bulk solution and 't' is the irradiation reaction time) will lead to the following expected relationship from equation (7).

$$\ln(c_0/c_t) = k_{app}t \quad (7)$$

Where, ' c_t ' and ' c_0 ' are the reactant concentrations at $t = t$ and $t = 0$, ' k_{app} ' and ' t ' are the apparent reaction rate constant and time respectively.

According to this equation, a plot of $\ln(c_0/c_t)$ versus UV light irradiation time (t) is drawn (Figs. 10 and 11). The apparent first-order constant is determined as 0.00209, 0.00334, 0.00442, 0.01302 for methyl orange (no catalysts), rhodamine B (no catalysts), methyl orange (10 mg catalysts) and rhodamine B (10 mg catalysts) respectively. Particularly, it is considered that the reaction rate of rhodamine B (10 mg catalysts) was good agreement with the results reported by others [44]. According to the above experimental data, the Co_3O_4 nanoparticle is having excellent photocatalytic activity towards the photodegradation of methyl orange and rhodamine B dyes under UV light irradiation.

4. Conclusions

Co_3O_4 nanoparticles are prepared by reflux condensed method using SDS and the results are reported. The XRD data obtained on Co_3O_4 nanoparticles shown that crystallized face-centered cubic in nature. The FTIR data confirmed the presence of Co-O bond and confirmed the formation of Co_3O_4 spinel oxide. The particle size of Co_3O_4 particles present in the range 43 nm. The SEM photograph confirmed the presence of nano sized as well as few micron sized grains in the sample. The EDAX data confirmed the presence of two elements (cobalt and oxygen) in the samples. The optical absorption band gap of the Co_3O_4 nanoparticles was found to be 5.6 eV, which is comparably more than that of reported data. Photocatalytic activity of the Co_3O_4 nanoparticles investigated in methyl orange and rhodamine B dyes under UV light irradiation (for two hours) resulted in the degradation of 76% and 74% respectively. Therefore, Co_3O_4 nanoparticles are found to be very promising materials for the degradation of organic matter present effluents discharged by small or large scale industries.

Acknowledgment

The authors are grateful to the DST Nano Mission, Govt. of India and New Delhi to carry out the research work. ASN thanks the management of Karunya University for its support to carry-out this research work in the Department of Chemistry and publish the same.

References

- [1] D.D. Liu, H. Wu, R. Zhang, W. Pan, Chem. Mater. 21 (2009) 3479-3484.
- [2] F. Xia, E. Ou, L. Wang, J. Wang, Dyes Pigments 76 (2008) 76-81.
- [3] H. Pouretedal, M. Ahmadi, Iran. J. Catal. 3 (2013) 149-155.
- [4] H. Faghihian, A. Bahrani-fard, Iran. J. Catal. 1 (2011) 45-50.
- [5] A. Bagheri Ghomi, V. Ashayeri, Iran. J. Catal. 2 (2012) 135-140.
- [6] M.H. Habibi, E. Askari, Iran. J. Catal. 1 (2011) 41-44.
- [7] A. Nezamzadeh-Ejhieh, M. Khorsandi, Iran. J. Catal. 1 (2011) 99-104.
- [8] H. Pouretedal, S. Basati, Iran. J. Catal. 2 (2012) 51-55.
- [9] A. Nezamzadeh-Ejhieh, Z. Banan, Iran. J. Catal. 2 (2012) 79-83.
- [10] G. Wang, X. Shen, J. Horvat, B. Wang, H. Liu, D. Wexler, J. Yao, J. Phys. Chem. C. 113 (2009) 4357-4361.
- [11] Mocuta, A. Barbier, G. Renaud, Appl. Surf. Sci. 56 (2000) 162-163.
- [12] H. Yamamoto, S. Tanaka, T. Naito, K. Hirao, Appl. Phys. Lett. 81 (2002) 999-1001.
- [13] X. Yao, X. Xin, Y. Zhang, J. Wang, Z. Liu, X. Xu, J. Alloys Compd. 521 (2012) 95-100.
- [14] J.S. Park, X.P. Shen, G.X. Wang, Sensors Actuat. B: Chem. 136 (2009) 494-498.
- [15] V.R. Mate, M. Shirai, C.V. Rode, Catal. Commun. 33 (2013) 66-69.
- [16] Y. Cui, Z. Wen, S. Sun, Y. Lu, J. Jin, Solid State Ion. 225 (2012) 598-603.
- [17] S.K. Meher, G.R. Rao, J. Phys. Chem. C. 115 (2011) 25543-25556.
- [18] B. Solsona, T.E. Davies, T. Garcia, A. Dejoz, S.H. Taylor, Appl. Catal. B: Environ. 84 (2008) 176-184.
- [19] A. Askarinejad, A. Morsali, Ultrason. Sonochem. 16 (2009) 124-131.
- [20] V.R. Shinde, S.B. Mahadik, T.P. Gujar, C.D. Lokhande, Appl. Surf. Sci. 252 (2006) 7487-7492.
- [21] B. Varghese, Y. Zhang, L. Dai, V.B.C. Tan, C.T. Lim, C.H. Sow, Nano Lett. 8 (2008) 3226-3232.
- [22] Y. Zhang, Y. Chen, J. Zhou, T. Wang, Y. Zhao, Solid State Commun. 149 (2009) 585-588.
- [23] T. Lai, Y. Lai, C. Lee, Y. Shu, C. Wang, Catal. Today 131 (2008) 105-110.

- [24] F. Svegl, B. Orel, M.G. Hutchins, K. Kalcher, J. Electrochem. Soc. 143 (1996) 1532-1539.
- [25] S. Noguchi, M. Mizuhashi, Thin Solid Films 77 (1981) 99-106.
- [26] M.E. Baydi, G. Poillerat, J.L. Rehspringer, J.L. Gautier, J.F. Koenig, P. Chartier, J. Solid State Chem. 109 (1994) 281-288.
- [27] L. Li, Y. Chu, Y. Liu, J.L. Song, D. Wang, X.W. Du, Mater. Lett. 62 (2008) 1507-1510.
- [28] Venkatesvara, K. Rao, C.S. Sunandana, Solid State Commun. 148 (2008) 32-37.
- [29] J.C. Toniolo, A.S. Takimi, C.P. Bergmann, Mater. Res. Bull. 45 (2010) 672-676.
- [30] S.M.I. Morsy, S.A. Shaban, A.M. Ibrahim, M.M. Selim, J. Alloys. Comp. 486 (2009) 83-87.
- [31] D.Y. Kim, S.H. Ju, H.Y. Koo, S.K. Hong, Y.C. Kangf, J. Alloys Comp. 417 (2006) 254-258.
- [32] Rumplecker, F. Kleitz, E.L. Salabas, F. Schüth, Chem. Mater. 19 (2007) 485-496.
- [33] F. Mohandes, F. Davar, M. Salavati-Niasari, J. Magn. Mater. 322 (2010) 872-877.
- [34] A.S. Bhatt, D.K. Bhat, C.W. Tai, M.S. Santosh, Mater. Chem. Phys. 125 (2011) 347-350.
- [35] X. Wang, X.Y. Chen, L.S. Gao, H.G. Zheng, Z. Zhang, Y.T. Qian, J. Phys. Chem. B. 108 (2004) 16401-16404.
- [36] Y. Zhang, Y. Liu, S. Fu, F. Guo, Y. Qian, Mater. Chem. Phys. 104 (2007) 166-171.
- [37] X. Ke, J. Cao, M. Zheng, Y. Chen, J. Liu, G. Ji, Mater. Lett. 61 (2007) 3901-3903.
- [38] W. Zhang, H.L. Tay, S.S. Lim, Y. Wang, Z. Zhong, R. Xu, Appl. Catal. B: Environ. 95 (2010) 93-99.
- [39] Q.J. H. Choi, Y.J. Chen, D.D. Dionysiou, Appl. Catal. B: Environ. 77 (2008) 300-307.
- [40] Q.J. Yang, H. Choi, D.D. Dionysiou, Appl. Catal. B: Environ. 74 (2007) 170-178.
- [41] X.Y. Chen, J.W. Chen, X.L. Qiao, D.G. Wang, X.Y. Cai, Appl. Catal. B: Environ. 80 (2008) 116-121.
- [42] M.A. Kanjwal, F.A. Sheikh, N.A.M. Barakat, Xiaoqiang Li, H. Yong Kim, I.S. Chronakis, J. Nanoeng. Nanomanuf. 1 (2011) 196-202.
- [43] F.H.B. Lima, M.L. Calegario, E.A. Ticianelli, J. Electroanal. Chem. 590 (2006) 152-160.
- [44] L.H. Ai, J. Jiang, Powder Technol. 195 (2009) 11-14.
- [45] Venkataraman, V.A. Hiremath, S.K. Date, S.D. Kulkarni, Bull. Mater. Sci. 24 (2001) 101-104.
- [46] A. Kodge, S. Kalyani, A. Lagashetty, Int. J. Eng. Sci. Technol. 3 (2011) 6381-6390.
- [47] C.N.R. Rao: Chemical Applications of Infrared Spectroscopy, Academic Press, NewYork, London, 1963.
- [48] Z.P. Xu, H.C. Zeng, J. Mater. Chem. 8 (1998) 2499-2506.
- [49] B. Pejova, A. Isahi, M. Najdoski, Mater. Res. Bull. 36 (2001) 161-170.
- [50] T. Koutzarova, S. Kolev, C. Ghelev, D. Paneva, I. Nedkov, Phys. Stat. Sol. C. 3 (2006) 1302-1307.
- [51] Gulino, P. Dapporto, P. Rossi, I. Fragala, Chem Mater. 15 (2003) 3748-3752.
- [52] F. Gu, C. Li, Y. Hu, L. Zhang, J. Cryst. Growth 304 (2007) 369-373.
- [53] R. Xu, H.C. Zeng, Langmuir 20 (2004) 9780-9790.
- [54] R.M. Mohamed, E.S. Baeissa, I.A. Mkhaliid, M.A. Al-Rayyani, Appl Nanosci. 3 (2013) 57-63.
- [55] S.S. Hong, M.S. Lee, J.H. Kim, B.H. Ahn, K.T. Lim, G.D. Lee, J. Ind. Eng. Chem. 8 (2002) 150-159.